http://www.lbl.gov/Science-Articles/Archive/quasicrystal-states.html

Strange Quasicrystal Alloys Spring Electronic Surprise On Researchers

Paul Preuss, paul_preuss@lbl.gov

BERKELEY, CA An international team of scientists has demonstrated that the electronic states of the strange metal alloys known as quasicrystals are more like those of ordinary metals than theorists believed possible.

Eli Rotenberg, a staff scientist at the Advanced Light Source (ALS) at the Department of Energy's Lawrence Berkeley National Laboratory, Karsten Horn of the Fritz-Haber Institute, Max-Planck Society, Berlin, and their colleagues investigated the electronic structure of a quasicrystalline alloy of aluminum-nickel-cobalt (AlNiCo) by means of angle-resolved photoemission. They report their findings in the August 10 issue of the journal *Nature.*

They found that rather than moving around arbitrarily, electrons in quasicrystals travel in "bands" with distinct momentum and energy. The data show that electron momenta and energies are correlated with the structure of the quasicrystal.

Band-like properties, common in metals and other ordinary crystals, were not expected in quasicrystals. But then quasicrystals themselves are an unexpected phenomenon.

"Before quasicrystals were discovered by Dan Schechtman and his colleagues in 1984, most people would have said they were structurally impossible," says Rotenberg. "You can tile a plane with equilateral triangles or squares -- shapes with three-fold or four-fold rotational symmetry -- and you can fill space periodically with tetrahedrons or cubes, which are two of the ways that atoms are typically arranged in ordinary crystals. But you can't tile a plane with pentagons -- not without leaving gaps -- and you can't fill space with dodecahedrons."

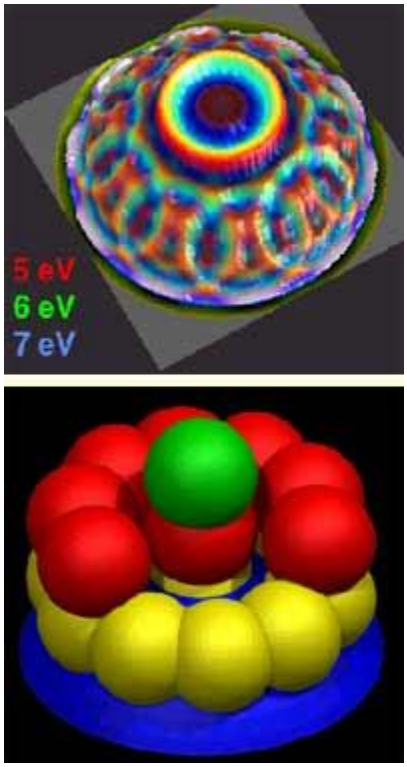

THE CONSTANT ENERGY CONTOURS FOR NEARLY FREE S-P ELECTRONS IN AlNiCo QUASICRYSTALS (DATA, TOP) ARE DERIVED FROM THREE-DIMENSIONAL SPHERES DISTRIBUTED APERIODICALLY IN MOMENTUM SPACE (MODEL, BOTTOM).

Yet, although quasicrystals display five-fold symmetry and other "forbidden" symmetries locally, they still possess perfect long-range structural order. So complex is their geometry that it has taken years to understand how their long-range atomic structures could arise.

Other investigations have centered on potentially useful properties. Quasicrystalline alloys are durable, stable at high temperatures, and make excellent nonstick coatings -- and they can store hydrogen at high density.

Though they are composed of excellent electrical conductors such as aluminum and copper, quasicrystalline alloys themselves are extremely resistive -- the more perfect the quasicrystal, the more resistive it becomes. At low temperatures their resistance changes markedly in

response to changing magnetic fields, which makes them interesting for applications in magnetic devices.

"But few experiments have been done on the basic properties of their electronic states," says Rotenberg. "In other words, where are the electrons and how do they move? These were unresolved questions."

Ordinary metals are good conductors because their valence electrons can move freely from atom to atom; this freedom is facilitated by long-range periodic structure. Since quasicrystals lack periodic structure, theorists expected no such extended electronic states.

"**One might imagine that from an electron's point of view the material appears disordered**. If so, the electronic states would be confined to localized clusters," Rotenberg says, and indeed, theoretical considerations suggested electronic states confined to the quasicrystal's many different local structures.

Rotenberg, Horn, and their colleagues decided to test the prediction with **a special kind of quasicrystal, an AlNiCo alloy consisting of stacked planes of atoms exhibiting ten-fold symmetry.** By looking at the behavior of electrons in the plane, they could observe the effects of this quasicrystalline ordering; by looking at right angles to the planes, they could observe the effects of the periodic, crystalline-like ordering of the stack.

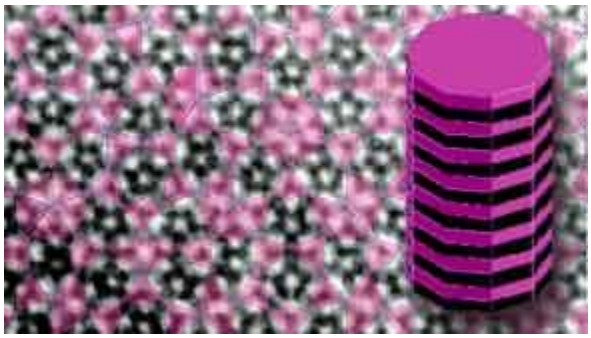

IN THE PLANE, THE AlNiCo QUASICRYSTAL, WHICH CONSISTS OF OVERLAPPING DECAGONS, IS APERIODIC. BUT THE STACKED PLANES HAVE PERIODIC STRUCTURE.

Images by Steinhardt and Jeong, Nature 382, 433-5

Peter Gille of the Ludwig-Maximilians-University, Munich, grew the quasicrystal, and the samples were prepared and characterized by Horn and by Wolfgang Theis of the Free University of Berlin. At the ALS, Rotenberg, Horn, and Theis examined the samples by means of low-energy electron diffraction and by angle-resolved photoemission at beamline endstation 7.0.1.2.

"We measure the emission angles and the kinetic energy of electrons

scattered from near the surface of the material by soft x rays," says Rotenberg. "These are the valence electrons, not as tightly bound as electrons near the atomic cores."

The sample is rotated to get a complete distribution of electron angles and energies. The eventual result is a plot of the electronic states of AlNiCo's valence electrons in "momentum space," the mathematical space in which such fundamental concepts as Fermi surfaces and Brillouin zones are constructed and on which much of the band theory of solids is based.

"Our principal findings were that the distribution of the electronic states in momentum space correlates with the electron diffraction pattern, just like in an ordinary crystal. **The electrons aren't localized to clusters, instead they feel the long-range quasicrystal potential," Rotenberg says.**

"We found that the electrons propagate nearly freely, like conduction electrons in an ordinary metal," he continues, "and we found there is a Fermi surface, crossed by nickel and **cobalt d-electrons**; **its topology should determine some of the material's fundamental properties."**

The discoveries open many new avenues for inquiry, Rotenberg says. **"How can we relate our observations to unusual properties such as high resistivity? And are there any localized electrons in addition to the delocalized electrons we found that look so 'ordinary?'"**

"Quasicrystalline valence bands in decagonal AlNiCo," by Eli Rotenberg, Wolfgang Theis, Karsten Horn, and Peter Gille appears in *Nature*, 10 August 2000.

The Berkeley Lab is a U.S. Department of Energy national laboratory located in Berkeley, California. It conducts unclassified scientific research and is managed by the University of California.

Surface Science

Volumes 454–456, 20 May 2000, Pages 453–457

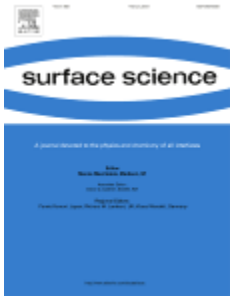

Electronic characterization of quasicrystalline surface transformations

- A. Hensch,
- B. Bolliger,
- M. Erbudak,
- R.F. Willis[1]
- Laboratorium für Festkörperphysik, Eidgenössische Technische Hochschule Zürich, CH-8093 Zürich, Switzerland

- http://dx.doi.org/10.1016/S0039-6028(00)00218-1, How to Cite or Link Using DOI

http://www.sciencedirect.com/science/article/pii/S0039602800002181

Origin of the Hall-coefficient anisotropy in the Y–Al–Ni–Co periodic approximant to the decagonal phase

- M. Komelj[a],
- J. Ivkov[b],
- A. Smontara[b],
- P. Gille[c],
- P. Jeglič[a],
- J. Dolinšek[a],
- [a] J. Stefan Institute, University of Ljubljana, Jamova 39, SI-1000 Ljubljana, Slovenia
- [b] Institute of Physics, Laboratory for the Study of Transport Problems, Bijenička 46, POB 304, HR-10001 Zagreb, Croatia
- [c] Ludwig-Maximilians-Universität München, Department of Earth and Environmental Sciences, Crystallography Section, Theresienstrasse 41, D-80333 München, Germany

- http://dx.doi.org/10.1016/j.ssc.2009.01.013, How to Cite or Link Using DOI
- Permissions & Reprints

Abstract

We present an experimental and theoretical study of the anisotropic Hall coefficient R_H of the Y–Al–Ni–Co periodic approximant to the decagonal phase with composition $Al_{76}Co_{22}Ni_2$. Performing *ab-initio* calculation of R_H for the original Y–Al–Ni–Co structural model [B. Zhang, V. Gramlich, W. Steurer, Z. Kristallogr. 210 (1995) 498] and its relaxed version, we reproduced the experimentally observed anisotropy for all combinations of crystalline directions of the electric current and magnetic field, where the relaxed model yielded better quantitative matching to the experiment. The origin of the anisotropic Hall coefficient is the anisotropic Fermi surface, the anisotropy of which originates from the specific stacked-layer structure of the Y–Al–Ni–Co compound and the chemical decoration of the lattice. Due to the structural similarity of Y–Al–Ni–Co to the *d*-Al–Ni–Co-type decagonal quasicrystals, the same physical picture explains the universal $R_H$anisotropy of this family of quasicrystals, where R_H changes sign along different crystalline directions.

PACS

- 61.44.Br;
- 71.23.Ft

Keywords

- A. Complex intermetallics;
- A. Quasicrystalline approximants;
- D. Electronic transport;
- D. Hall effect

Figures and tables from this article:

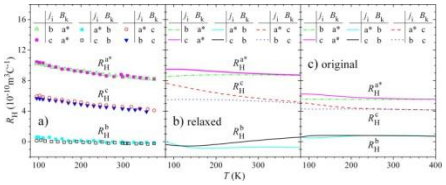

Fig. 1. (Color online) (a) Experimental anisotropic temperature-dependent Hall coefficient $R_H^{ilm} = E_l / j_i B_m$ of Y–Al–Ni–Co for different combinations of directions of the current j_i and magnetic field B_m (given in the legend). The superscript *a*, *b* or *c* on R_H denotes the direction of the magnetic field, whereas the indices *i*, *l* are omitted. (b) Theoretical anisotropic Hall coefficient for the same set of current and field directions as in (a). R_H was calculated *ab-initio* using the relaxed structural model of the Y–Al–Ni–Co phase of composition $Al_{75}Co_{25}$. (c) Theoretical anisotropic Hall coefficient calculated along the same lines as in (b), by using the original Zhang et al. [5] structural model of Y–Al–Ni–Co.

Figure options

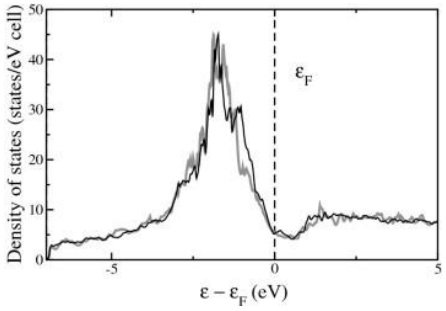

Fig. 2. Theoretical electronic DOS of the Y–Al–Ni–Co phase, calculated *ab-initio* for the original structural model of Zhang et al. [5] (thick grey curve) and the relaxed model (thin black curve), assuming composition $Al_{75}Co_{25}$. The DOS of the original model is reproduced from Ref. [4].

Figure options

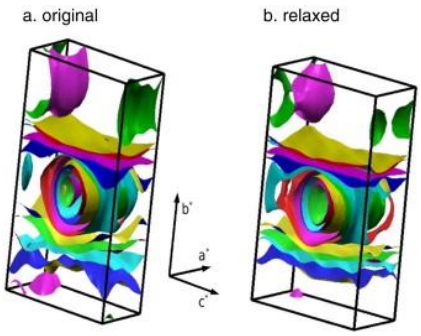

Fig. 3. (Color online) Fermi surface in the first Brillouin zone, calculated *ab-initio* for (a) the original Y–Al–Ni–Co model (Zhang et al. [5]) of composition $Al_{75}Co_{25}$ and (b) its relaxed version. Orientation of the reciprocal-space axes a^*, b^* and c^* is also shown. While a^* and c^* are perpendicular to b^*, the angle between a^* and c^* amounts 63.83°. The Fermi surface of the original model is reproduced from Ref. [4].

Figure options

Table 1. Fractional atomic coordinates (x, y, z) of the relaxed model of Y–Al–Ni–Co. The coordinates (xZ, yZ, zZ) of the original model of Zhang et al. [5] are given for comparison. The labels of the atomic positions together with their Wyckoff positions and site symmetry follow the labeling of Ref. [5] and TM denotes transition metal.

View Within Article

http://www.sciencedirect.com/science/article/pii/S0038109809000271

ELSEVIER

Physica B: Condensed Matter

Volume 407, Issue 5, 1 March 2012, Pages 827–832

Electronic structure of single crystal and highly oriented pyrolytic graphite from ARPES and KRIPES

- R. Kundu[a],
- P. Mishra[a],
- B.R. Sekhar[a],

- M. Maniraj[b],
- S.R. Barman[b]
- [a] Institute of Physics, Sachivalaya Marg, Bhubaneswar 751005, India
- [b] Surface Physics Laboratory, UGC-DAE Consortium for Scientific Research, Khandwa Road, Indore 452001, Madhya Pradesh, India

- http://dx.doi.org/10.1016/j.physb.2011.12.013, How to Cite or Link Using DOI

Abstract

We present a comparative study of the near fermi-level electronic structure of single crystal and highly oriented pyrolytic graphite (HOPG). Angle resolved photoelectron spectroscopy and angle resolved inverse photoelectron spectroscopy have been used to probe the occupied and unoccupied electronic states, respectively. The band dispersions showed by single crystal graphite along its Γ*K* and Γ*M* symmetry directions were found to be in agreement with calculated band structure of graphite. The π bands of single crystal graphite were found to have a splitting of $\sim 0.5\,\mathrm{eV}$ at the *K*-point. We also observe the presence of a quasiparticle peak below E_F at the *K* point at low temperature which indicates a strong electron–phonon coupling in graphite. In HOPG, the *M* and *K* points like features were found to be present in the same radial direction due to the superposition of the Γ*M* and Γ*K* directions. Results from our angle resolved inverse photoemission spectroscopy present the dispersion of the conduction band states, particularly the lower π□band. We have also found the presence of some non-dispersive features in both the valence and the conduction bands.

Keywords

- ARPES;
- KRIPES;
- Graphite;
- HOPG;
- Band structure

Figures and tables from this article:

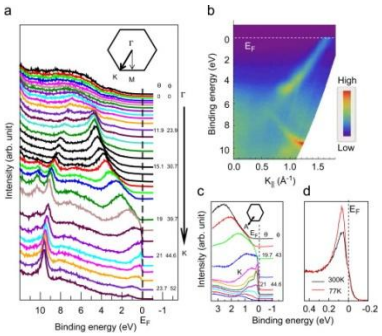

Fig. 1. (a) The raw photoemission data from single crystal graphite along the Γ*K* direction of its Brillouin zone. Shown in the inset is the two dimensional Brillouin zone of graphite. The emission angles θ and ϕ (in degree) for some of the spectra are indicated beside the spectra. In (b) the photoemission intensity plot as a function of binding energy and $k_{||}$ derived from the spectra in (a) is shown. The spectra along the cut A of the Brillouin zone through the *K* point over a small energy range near Fermi energy are shown in (c). In (d) the spectra over a very small energy range at the *K* point at two different temperatures (300 K (black curve) and 77 K (red curve)) are compared. (For interpretation of the references to color in this figure legend, the reader is referred to the web version of this article.)

Figure options

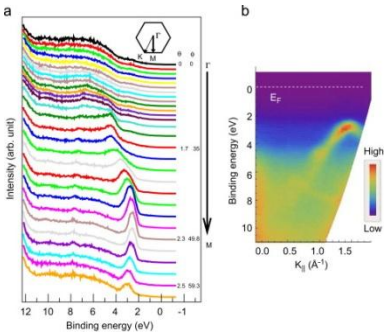

Fig. 2. (a) The spectra along the Γ*M* direction of graphite Brillouin zone. The emission angles for some of the spectra are marked beside the spectra. (b) The intensity map of the spectra shown in (a) as a function of binding energy and $k_{||}$.

Figure options

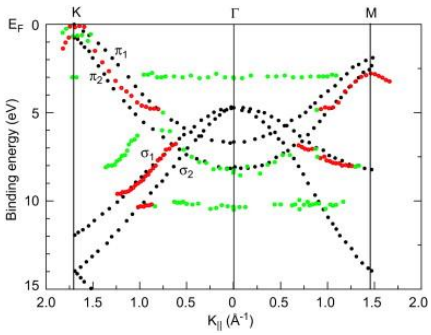

Fig. 3. Energy versus momentum component parallel to the sample surface ($E(k) \sim k_{||}$) for all the strong (red circles) and weak (green circles) peaks of the experimental results in Fig. 1 and Fig. 2. They have been plotted along with a theoretical band structure (black circles) of graphite in the Γ*K* and Γ*M* directions of the Brillouin zone. (For interpretation of the references to color in this figure legend, the reader is referred to the web version of this article.)

Figure options

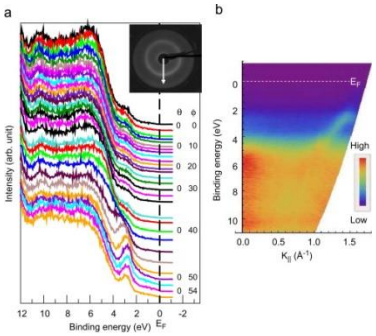

Fig. 4. (a) The angle resolved photoemission spectra of HOPG along a radial direction of the circular Brillouin zone (along the arrow shown in inset); the low energy electron diffraction pattern of HOPG was taken at room temperature with a beam energy of 165 eV. The circular pattern, instead of six distinct spots as in single crystal graphite, shows its quasicrystalline structure. Since different symmetry directions of the Brillouin zone get averaged out, all the radial directions become equivalent. (b) The intensity plot of the photoemission spectra shown in (a).

Figure options

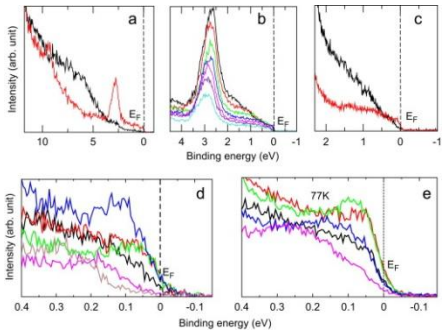

Fig. 5. Spectra of HOPG along the same direction as in Fig. 4 over different energy ranges: (a) shows the spectra at the Γpoint (black curve) and at the zone boundary (red curve) over an energy range of $\sim 11\ \mathrm{eV}$, (b) shows a set of spectra at and around the zone boundary over an energy range of $\sim 5\ \mathrm{eV}$, in (c) the spectra at *K* point (red curve) and slightly away from the *K* point (black curve) of the Brillouin zone over the energy range of ~ 3 eV are compared. The *K* point spectra shows the appearance of a small peak very close to the Fermi energy. The dispersion of this peak for some nearby angles is shown in (d) where the spectra are taken over an energy range of 0.5 eV, the same taken at a temperature of 77 K is shown in (e). (For interpretation of the references to color in this figure legend, the reader is referred to the web version of this article.)

Figure options

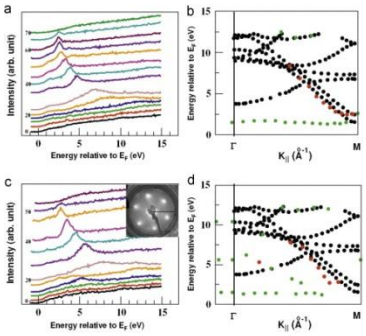

Fig. 6. (a) The *k*-resolved inverse photoemission spectra of HOPG along a radial direction; (c) the same taken on single crystal graphite along the direction shown in inset. It is ~17° away from the Γ–*M* direction of the Brillouin zone of graphite. The spectra were taken at an interval of 5°. For clarity, polar angle of incident electrons referred to the surface normal for some of the spectra are marked beside. All the strong (red circles) and weak (green circles) peaks of the experimental results in (a) and (c) have been plotted in (b) and (d), respectively, along with the theoretical (black circles) unoccupied bands of graphite calculated by Holzwarth et al. [29] in the Γ–*M* direction of the Brillouin zone. (For interpretation of the references to color in this figure legend, the reader is referred to the web version of this article.)

Figure options

Corresponding author. Tel.: +91 6742301058; fax: +91 6742300142.

1. Electronic structure, density of states and properties of quasicrystals
2. 1999, Current Opinion in Solid State and Materials Science
3. Show more information
2. View more articles »
Cited by in Scopus (0)

Related reference work articles

1.
1. Carbon Nanotubes: Electronic Structure and Physical Properties
2. 2006, Encyclopedia of Materials: Science and Technology (Second Edition)
3. Show more information
2.
1. Quasicrystals, Electronic Structure of
2. 2005, Encyclopedia of Condensed Matter Physics
3. Show more information
3.
1. Semiconductor Optics
2. 2005, Encyclopedia of Condensed Matter Physics
3. Show more information
4. View more articles »

Share

Workspace

ELSEVIER

Current Opinion in Solid State and Materials Science

Volume 4, Issue 3, June 1999, Pages 295–301

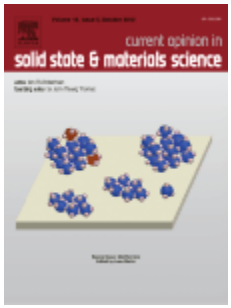

Electronic structure, density of states and properties of quasicrystals

- Takeo Fujiwara
- Department of Applied Physics, University of Tokyo, Bunkyo-ku, Tokyo 113, Japan

- http://dx.doi.org/10.1016/S1359-0286(99)00031-5, How to Cite or Link Using DOI
- Permissions & Reprints

View full text

Abstract

One of the recent important developments in solid state physics in the last 15 years is certainly the discovery of quasicrystals. Quasicrystal is the new thermodynamically stable state, in which the atomic arrangement is neither periodic nor random. Not only the structural arrangement, but also the electronic structures and properties are quite exotic. Several quasicrystals show an electric conductivity smaller than Mott's minimum metallic conductivity and the temperature coefficient of conductivity is large and negative. Lots of new information is still being collated.

Figures and tables from this article:

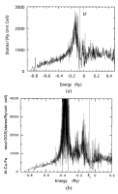

Fig. 1. Total DOSs of (a) Al–Mn (Reprinted from Physical Review B 1989;40:942, with permission from the American Physical Society.) [26] and (b) Al–Cu–Fe (Reprinted from Physical Review B 1994;50:5999, with permission from the American Physical Society.) [28].

Figure options

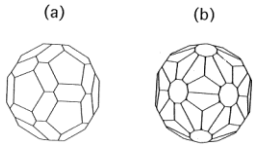

Fig. 2. The *pseudo*-Brillouin zone in quasicrystals. (a) *Pseudo*-BZ constructed from the [211111] and [221001] planes (MI-type), and (b) that from the [222100] and [311111]/[222110] planes (TC-type).

Figure options

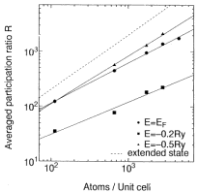

Fig. 3. The participation ratio of *d*-AlCuCo averaged over about 50 eigenstates near the Fermi energy E_F (•), 0.2 Ry below E_F(■), and 0.5 Ry below E_F (▲), as a function of the number of atoms, N, in a unit cell. (Reprinted from Physical Review B 1996;53:R2910, with permission from The American Physical Society.)

Figure options

Table 1. Classification of quasicrystals

View Within Article

Table 2. Reciprocal lattice vectors and the corresponding critical valence per atom (m_i denotes the six-dimensional components of the reciprocal lattice vectors [43])

View Within Article

Tel.: +81-3-5841-6810; fax: +81-3-5689-8254

Tel.: +81-3-5841-6810; fax: +81-3-5689-8254

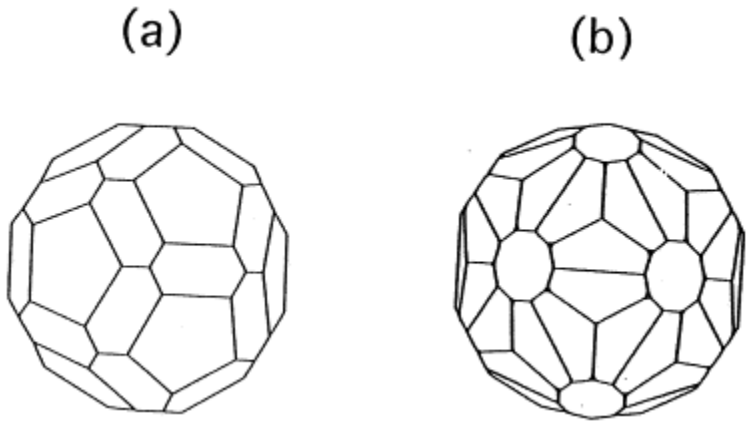

Fig. 2. The *pseudo*-Brillouin zone in quasicrystals. (a) *Pseudo*-BZ constructed from the [211111] and [221001] planes (MI-type), and (b) that from the [222100] and [311111]/[222110] planes (TC-type).

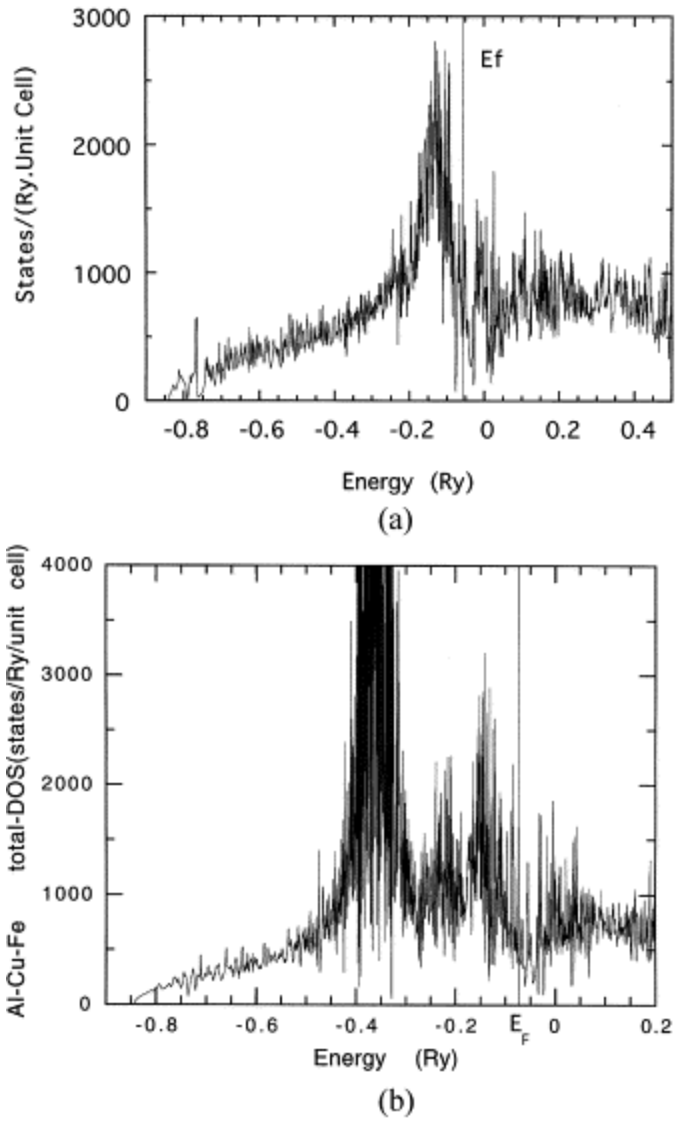

Fig. 1. Total DOSs of (a) Al–Mn (Reprinted from Physical Review B 1989;40:942, with permission from the American Physical Society.) [26] and (b) Al–Cu–Fe (Reprinted from Physical Review B 1994;50:5999, with permission from the American Physical Society.) [28].

http://ars.els-cdn.com/content/image/1-s2.0-S1359028699000315-gr1.gif

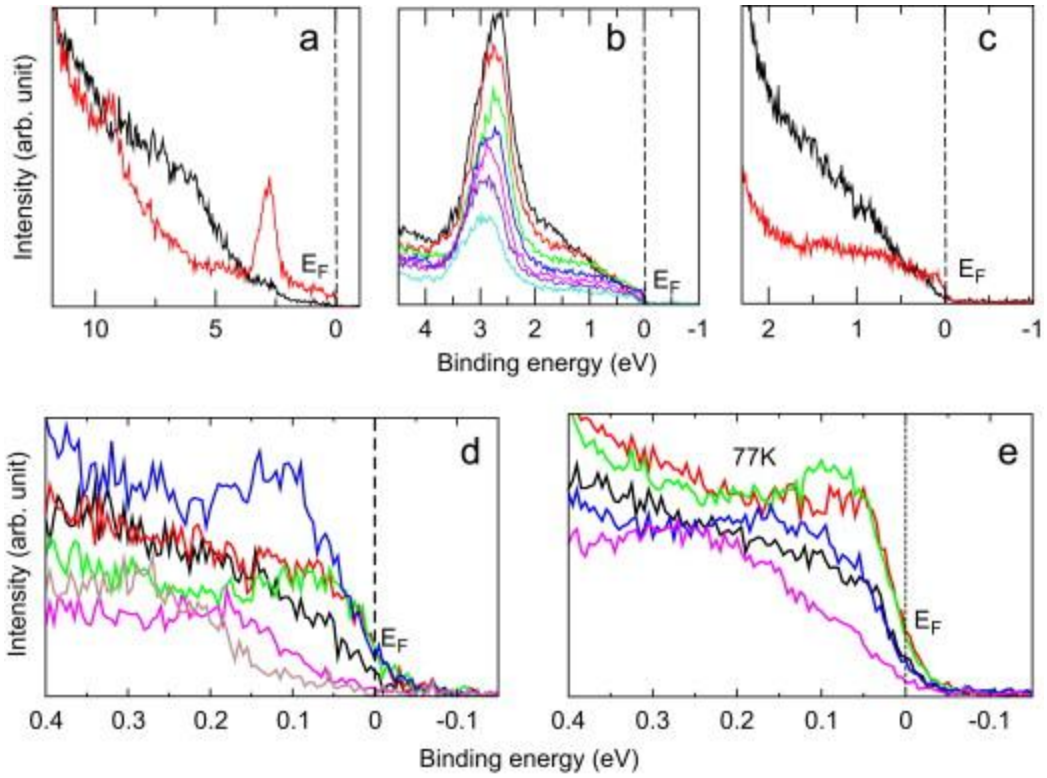

Fig. 5. Spectra of HOPG along the same direction as in Fig. 4 over different energy ranges: (a) shows the spectra at the Γpoint (black curve) and at the zone boundary (red curve) over an energy range of $\sim 11\ \mathrm{eV}$, (b) shows a set of spectra at and around the zone boundary over an energy range of $\sim 5\ \mathrm{eV}$, in (c) the spectra at *K* point (red curve) and slightly away from the *K* point (black curve) of the Brillouin zone over the energy range of ~ 3 eV are compared. The *K* point spectra shows the appearance of a small peak very close to the Fermi energy. The dispersion of this peak for some nearby angles is shown in (d) where the spectra are taken over an energy range of 0.5 eV, the same taken at a temperature of 77 K is shown in (e). (For interpretation of the references to color in this figure legend, the reader is referred to the web version of this article.)

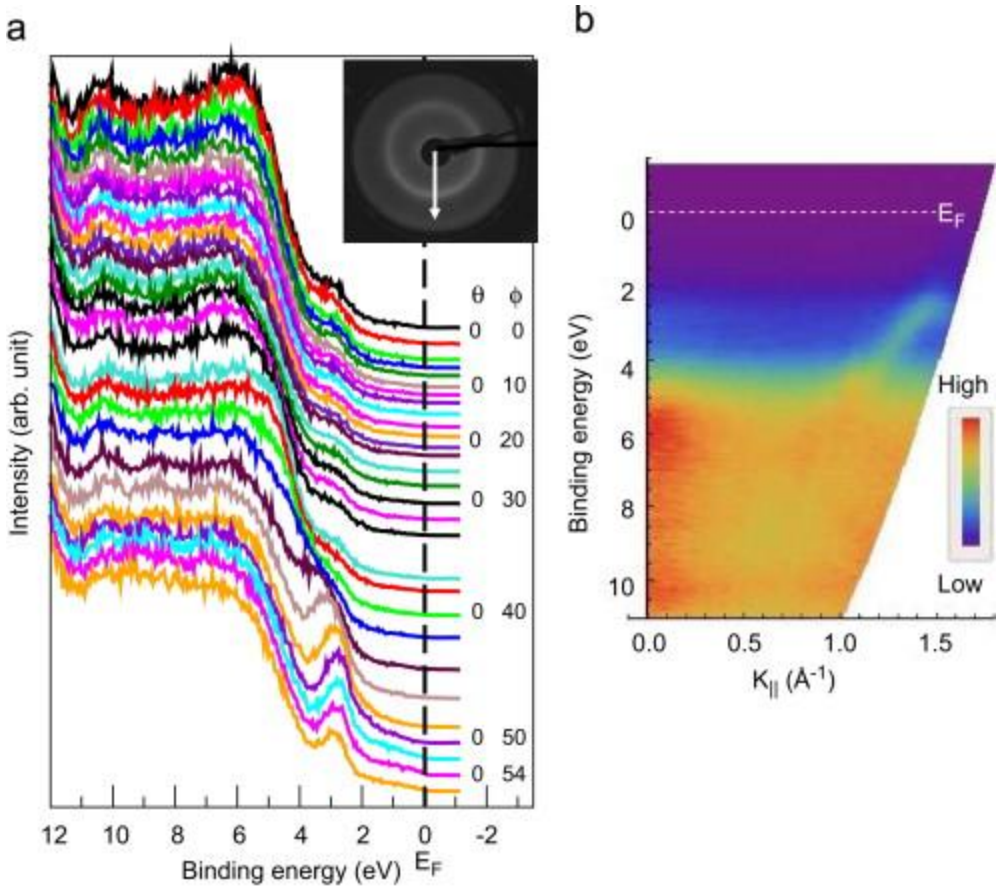

Fig. 4. (a) The angle resolved photoemission spectra of HOPG along a radial direction of the circular Brillouin zone (along the arrow shown in inset); the low energy electron diffraction pattern of HOPG was taken at room temperature with a beam energy of 165 eV. The circular pattern, instead of six distinct spots as in single crystal graphite, shows its quasicrystalline structure. Since different symmetry directions of the Brillouin zone get averaged out, all the radial directions become equivalent. (b) The intensity plot of the photoemission spectra shown in (a).

http://www.sciencedirect.com/science/article/pii/S0921452611011999